Journal of Engineering, Project, and Production Management
2026, 16(7), 2026-0052

Graph Neural Network Collaborative Optimization of Multi-Agent Cascade Hydropower Unit Combination under Spot Market Environment

Chang Xiao[1], Shumin Miao[2], Chi Zhang[3], Min Li[4], Lun Tang[5], Jiajia Wang[6], Lilin Peng[7], and Yanqiu Hou[8]
[1] Senior Engineer, State Grid Sichuan Electric Power Company, China, E-mail: xiaoc0013@sc.sgcc.com.cn (corresponding author).
[2] Senior Engineer, State Grid Sichuan Electric Power Company, China
[3] Senior Engineer, State Grid Sichuan Electric Power Company, China
[4] Senior Engineer, State Grid Sichuan Electric Power Company, China
[5] Senior Engineer, State Grid Sichuan Electric Power Company, China
[6] Senior Engineer, Sichuan Power Exchange Center Co., Ltd., China
[7] Senior Engineer, Sichuan Power Exchange Center Co., Ltd., China
[8] Senior Engineer, State Grid Sichuan Electric Power Company Economic Research Institute, Chengdu 610041, China

Project Management
Received May 8, 2026; revised June 18, 2026; accepted July 29, 2026
Available online August 12, 2026

Abstract: With the growing frequency of spot market transactions, cascade hydropower units are required to make rapid decisions in complex hydrological conditions, uncertain loads, and multi-agent strategic games. Traditional scheduling methods fall short in capturing the spatiotemporal coupling of cascade reservoirs and the high-dimensional structural information arising from the dynamic strategic feedback among multiple agents. To address this, this paper applies a graph neural network collaborative optimization framework with an enhanced multi-agent structure. First, a cascade hydropower unit combination relationship graph is constructed, and topological encoding is applied to features such as reservoir capacity, output, bidding price, and bidding characteristics for wind, solar, hydro, thermal, and storage. An interactive graph attention mechanism is designed to strengthen the influence of upstream and downstream and agent strategies. Subsequently, a time-series graph is used to embed a unified representation of the dynamic coupling features among price, hydrological conditions, and strategies, capturing the impact of wind and solar fluctuations, energy storage charging and discharging behavior, and changes in the marginal cost of thermal power on the clearing results. Furthermore, an end-to-end differentiable Graph Neural Network (GNN) fusion module for scheduling optimization is constructed, directly embedding the graph model output into cascade constraint optimization to achieve a joint solution of bidding clearing and cascade scheduling. Ultimately, a multi-objective collaborative learning strategy is employed to improve hydropower utilization, ensure compliance with safety constraints, and enhance multi-agent benefits, enabling the model to achieve higher collaborative decision-making capabilities and generalization performance in the spot market. Experiments show that the satisfaction rate of key constraints under typical operating conditions is above 0.8, and the hydropower bidding collaboration reaches 0.88 with a price fluctuation of only 2.3%, significantly better than wind power's 12.5%; the hydropower utilization efficiency during the normal water season reaches 92.8%, with a water abandonment rate as low as 1.2%; the safety margin in normal scenarios exceeds 15%, with a maximum safety score of 0.88, verifying the model's comprehensive advantages in collaborative decision-making, hydropower optimization, and safe operation.

Keywords: Spot market; cascaded hydropower; unit commitment optimization; graph neural network; collaborative optimization framework.

DOI 10.32738/JEPPM-2026-0053

---

1. Introduction

The continuous clearing process in the spot market gives rise to intensive bidding, rapid settlement, and multi-entity strategic interaction, thereby imparting significant time-varying attributes and strategic characteristics to power resource allocation. Wind, solar, hydro, thermal, and storage power sources submit bids based on cost structure, resource characteristics, and strategic expectations. The clearing results are continually evolving in response to supply and demand dynamics, price fluctuations, and strategic adjustments (Liu et al., 2024; Liu et al., 2023). Cascade hydropower is situated within a closely interconnected hydraulic regulation system, and its operation is jointly shaped by hydrological fluctuations, inflow uncertainty, reservoir capacity time-varying characteristics, unit operating conditions, and price stimuli (Zhai et al., 2024; Marcial and Perninge, 2023). The shortening of the spot market cycle has narrowed the decision-making period, making traditional, relatively static and linear scheduling methods difficult to adapt to the frequently changing market environment (Cai et al., 2022; Khodadadi et al., 2022). The hydraulic coupling between cascade reservoirs creates a linkage effect across different time periods, and cumulative bidding by multiple entities over continuous periods shifts price levels, resulting in scheduling that exhibits characteristics of high-dimensional interaction and strategic sensitivity (Ha et al., 2024; Bringedal et al., 2023).

Traditional models rely on fixed expressions of the structure of hydropower systems and on simplified assumptions about the behavior of multiple agents. They handle multi-source relationships separately and lack an accurate characterization of the interaction between the hydraulic structure and the strategy network in the spot market environment. The wind-solar deviation, the difference in marginal cost of thermal power, and the charging and discharging behavior of energy storage constantly rewrite the supply and demand relationship. The strategic adjustments of multiple agents form a continuous disturbance, putting pressure on the economy, safety and timeliness of cascade hydropower. Research on multi-agent cascade hydropower combination in the spot market environment is of great significance. Regarding power generation scheduling and resource allocation under spot market conditions, existing studies have developed various models focusing on multi-energy coordination, price response, electricity market behavior and the law of hydropower operation. Chen et al. (2024) proposed a market pricing model that accounts for the sufficiency of power generation capacity to address the capacity adequacy problem in multi-energy systems, providing a reference for the price formation mechanism in a multi-agent environment. On this basis, Kiene and Linkevics (2021) further explored a simplified evaluation method for converting conventional hydropower stations into pumped-storage power stations to improve the system's flexibility in adjustment. For power generation forecasting, Zhang et al. (2022) combined improved ensemble empirical mode decomposition with adaptive neural network switching to achieve high-precision hybrid forecasting of hydropower generation; meanwhile, Xie et al. (2022) used an extreme gradient boosting algorithm to forecast the clearing price of the day-ahead spot market, improving the tracking accuracy of price time series. In terms of trading strategies, Lu et al. (2022) examined the medium- and long-term strategies of large retailers in China's electricity market, offering insights into optimizing market participants' decisions. In addition, Bin (2021) explored the future development trajectory of hydropower in China, emphasizing its key role in the clean energy transition. Finally, Borges et al. (2023) focused on the coordinated operation of multi-ownership cascade hydropower systems and proposed a profit-sharing mechanism to coordinate different stakeholders. Although existing work has made progress in many aspects, there is still room for further research in dynamic decision-making, differentiability optimization and comprehensive assessment of safety margin in the coordination of cascade hydropower and multi-energy markets (Naversen et al., 2022; Kristiansen, 2023). Some studies have attempted to incorporate multi-agent parameters into hydropower dispatch models, making assumptions about the load-bearing ratio or price trends of other power sources to enable hydropower to adjust its output in response to external factors. However, such approaches struggle to capture the dynamic evolution of wind, solar, thermal, and energy storage strategies in real markets (Borenstein et al., 2023; Sengthongkham et al., 2021). In summary, existing research typically builds strong capabilities in specific areas but falls short of addressing the complex problem of "hydraulic structure coupling + multi-agent strategy interaction" under spot-market conditions, making it difficult to support in-depth decision-making.

In recent years, graph structure learning has received widespread attention in the study of complex systems. Some studies have used graph neural networks to model correlations among wind and solar output, grid-node coupling, and inter-power policy links, demonstrating their strong ability to capture structured information. In the field of hydropower dispatching, some works have attempted to construct the graph structure of hydropower stations and reservoirs, using node attributes to describe features such as output, reservoir capacity, and water level, and edge attributes to express hydraulic relationships, thereby improving the accuracy of traditional models in characterizing watershed coupling (Schindler et al., 2024; Li et al., 2025). During the same period, differentiable optimization techniques have gained attention in power system optimization scenarios. Researchers have embedded neural network outputs into differentiable constraint solvers, aiming to create an end-to-end framework that enables data-driven and optimization models to be updated collaboratively (Condemi et al., 2021; Chen et al., 2022). Some studies have applied such methods to scenarios such as unit combination, distributed dispatching, or energy management, using continuous processing to closely connect optimization solutions with neural network expressions, thereby providing the solution process with greater structural expressiveness and learning capabilities. However, there are still insufficient expressions in complex problems such as multi-agent bidding, cascade hydraulic coupling, and time-series policy transmission (Ding et al., 2021; Coban and Sauhats, 2022). Many studies neglect the interactive effects between multi-agent strategies when constructing graph structures, lack a structured expression of the coupling of wind, solar, hydro, thermal, and energy storage strategies in market modeling, and lack a unified description of the co-evolution of prices, water conditions, and strategies in time series inference, making it difficult for models to reflect the complex dynamics of the real spot market environment (Antonio Nunes et al., 2024; Pan et al., 2022; Zhang et al., 2025). Based on these shortcomings, it is necessary to explore a collaborative method that combines graph structure expression, time series relationship inference, multi-agent strategy transmission, and differentiable solution capabilities, in order to obtain a more suitable decision framework for cascade hydropower in a competitive clearing environment (Liao et al., 2021; Huang et al., 2024).

This study aims to construct a multi-agent cascade hydropower combination model suitable for spot-market environments, and to establish a novel methodological framework that describes hydraulic structures, market interactions, and strategy propagation. Therefore, this study explicitly explores the following core research question: Under the high-dimensional coupling of hydraulic constraints and spot market price fluctuations, how can a multi-agent cascade hydropower system dynamically optimize its unit combination and bidding strategies? To answer this question, it is hypothesized that combining topological graph representation with an end-to-end differentiable optimization framework can effectively capture the physical-hydraulic coupling and the dynamic strategy interactions among multiple energy agents. The main contributions in this paper are threefold. First, a novel topological modeling method is proposed that unifies hydraulic structures and multi-agent market strategies into a single graph representation. Second, an end-to-end differentiable graph neural network fusion module is developed to seamlessly integrate data-driven policy learning with physical cascade constraints. Third, a multi-objective collaborative learning mechanism is introduced to balance economic benefits, hydropower utilization, and system safety margin, providing a robust decision-making framework for the real-world spot market.

2. Collaborative Optimization Mechanism Design

To address the challenges of high-dimensional structure and dynamic strategies faced by cascade hydropower combinations in the spot market, this chapter systematically elaborates on a multi-agent collaborative optimization framework based on graph neural networks. As shown in Fig. 1, this framework comprises four core modules: a graph-structure modeling layer, a time-series graph-embedding layer, a differentiable fusion solution layer, and a multi-objective collaborative learning strategy.

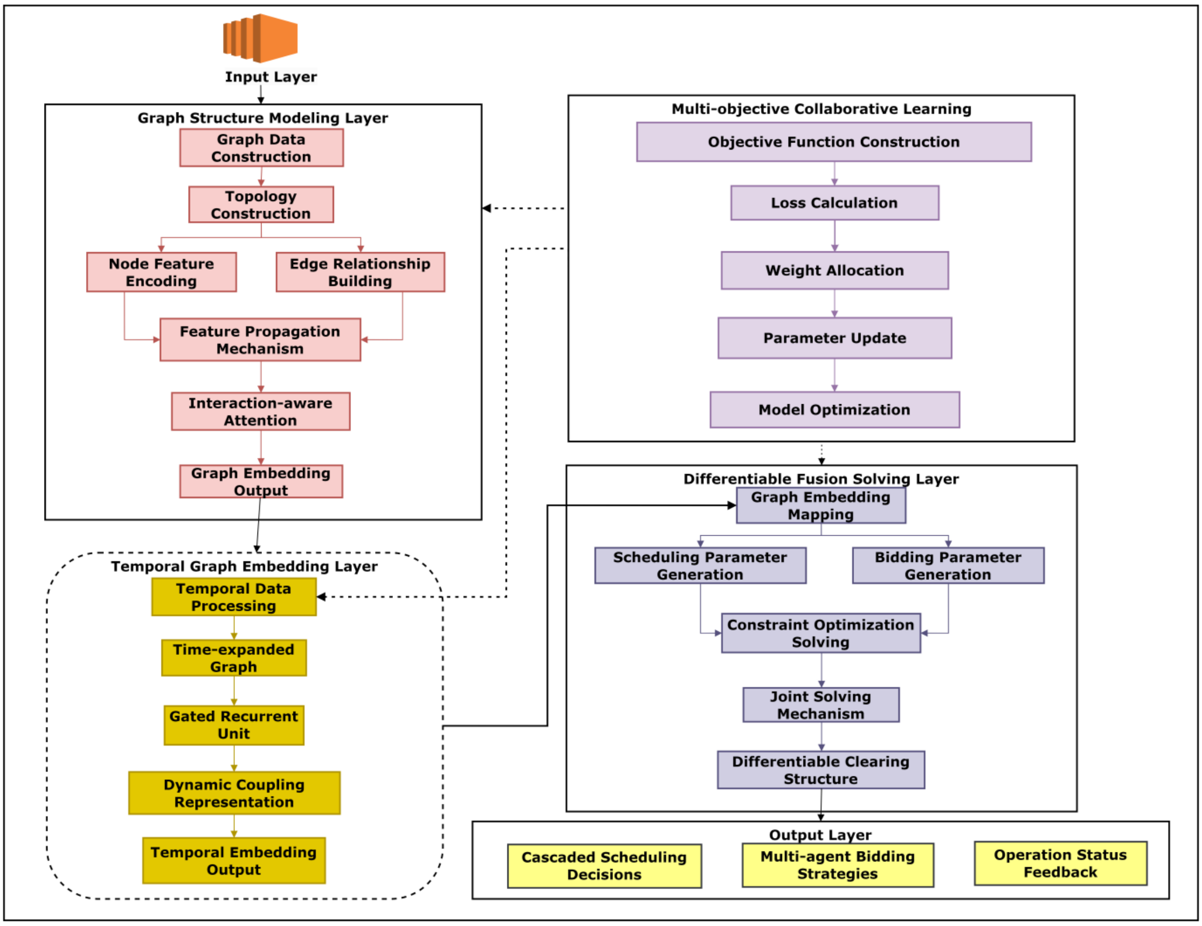

Fig.1. Framework for collaborative optimization of multi-agent cascade hydropower projects in a spot market

Fig. 1 illustrates the graph neural network method used to collaboratively optimize multi-agent cascade hydropower projects in a spot market. Its core process is as follows: first, a graph structure that incorporates hydraulic coupling and market interactions is constructed, and node relationships are enhanced via an attention mechanism. Second, temporal graph embedding is applied to capture dynamic features. Subsequently, the graph model output is combined with physical constraints via a differentiable optimization layer to obtain an end-to-end joint solution; finally, a multi-objective learning strategy jointly optimizes objectives such as economy, safety, and hydropower utilization, driving iterative updates of the entire model.

2.1. Multi-Subject Graph Structure Modeling of Cascade Hydropower

2.1.1. Topology construction and attribute mapping

The node set takes cascade reservoirs, power plant units, wind and solar power units, thermal power units and energy storage units as basic objects and establishes a unified node table across subjects through the topology index. The reservoir nodes are labeled with dynamic reservoir capacity $\mathrm{V_t}$, inflow $\mathrm{Q_t^{in}}$, outflow $\mathrm{Q_t^{out}}$, and available head $\mathrm{H_t}$, and written into the node attribute tensor in a continuous time series manner. The unit nodes are loaded with output range, ramp limit, start and stop status and price vector $\mathrm{b_t}$. The wind and solar nodes are assigned the predicted output sequence $\mathrm{P_t^{wp}}$ and correction factor as attributes; the thermal power nodes are assigned the marginal cost sequence, adjustable range and minimum start-up time; the energy storage nodes are assigned the state of charge S_t, charging and discharging power range and constraint matrix (Silinevicha, 2021). All attributes are normalized and assembled into a node feature matrix $X \in R^{N \times d}$.

The edge set is constructed based on the hydraulic channel, topology cascade and market interaction relationship. The hydraulic channel edges are constructed using reservoir-capacity connections and output-influence matrices to represent hydraulic relationships. Edge weights are weighted vectors based on head conversion coefficients, regulation time delays, and the contribution rate per unit discharge to downstream reservoirs. Wind, solar, thermal, and energy storage nodes are connected to hydropower nodes via bidirectional information edges reflecting market-strategy influence relationships. Edge weights are generated using bid change rates, clearing sensitivity, and reference price gradients. All edge weights form a weighted adjacency matrix A.

After topology construction, X and A are hierarchically written into the graph data structure. The hydraulic structure and market interaction structure are stored in different channels to ensure differentiated processing during propagation. This graph structure allows cascade coupling and multi-agent strategies to be uniformly embedded into the subsequent GNN model, thus avoiding the fragmentation problem caused by the separate processing of scheduling variables, market strategies, and hydrological correlations.

2.1.2. Graph feature propagation mechanism and multi-subject interactive encoding

Graph feature propagation is implemented using a channel-based attention structure. The propagation unit takes the node state h_i as input and calculates the attention weights for the hydraulic and strategy edges, respectively. The hydraulic attention mechanism takes the feature pairs composed of hydraulic variables such as reservoir capacity, discharge, and output as input and uses the trainable projection vector w_h to calculate the coefficients (Park et al., 2023), as shown in Eq. 1.

$$\alpha_{ij}^{hyd}=\mathrm{softmax}_j\left(\sigma(w_h^T|h_i||h_j||a_{ij}^{hyd}|\right) \tag{1}$$

where a_{ij}^{hyd} is the hydraulic edge weight. This structure strengthens the influence of upstream information on downstream units and reservoir capacity during propagation, and avoids the limitations of linear weights in expressing the asymmetric and time-delay characteristics of the hydraulic link. The strategy attention mechanism takes the bid vectors, output ranges and flexibility parameters of each subject as inputs and uses independent projection vectors w_s to encode the market interaction relationship (Ramesh and Li, 2023), resulting in Eq. 2.

$$\alpha_{ij}^{str}=\mathrm{softmax}_j\left(\sigma(w_s^T|h_i||h_j||a_{ij}^{str}|\right) \tag{2}$$

where a_{ij}^{str} is the strategy edge weight. This mechanism encodes the impact of multi-subject strategy changes on hydropower nodes and other nodes into the graph structure, so that strategy disturbances in the frequent bidding environment can be incorporated into the combinatorial solution process in a learnable way. The propagation results of the hydraulic channel and the strategy channel are weighted and combined and written into the node update, as shown in Eq. 3.

$$h_i^{'}=f\left(\sum_j \alpha_{ij}^{hyd} W_{hyd} h_j+\sum_j \alpha_{ij}^{str} W_{str} h_j\right) \tag{3}$$

where $f(\cdot)$ is a nonlinear mapping, and W_{hyd} and W_{str} They are trainable transformation matrices. This structure allows different types of information to enter the node state in a channel-separated learning manner, thereby avoiding gradient interference from mixing hydraulic relations and market strategies within the same parameter space (Li et al., 2023).

After propagation, the node state vector forms an embedded representation in the graph space that includes hydrological constraints, unit combination logic, and multi-agent strategy associations. This representation provides structured input for subsequent scheduling solutions and end-to-end joint training, enabling the coupling relationship of cascade hydropower under the clearing conditions of wind, solar, hydro, thermal, and storage bidding to be incorporated into the overall framework in a trainable manner.

Fig. 2 shows the visualization results of key features in multi-agent collaborative decision-making. In Fig. 2(a), the horizontal axis represents the feature dimensions, including storage capacity, output, price, head, ramp rate, and flexibility. The multi-agent number range N1 through N12 can be found on the vertical axis. The visual representation of different agents' physical limitations and operating characteristics is conveyed by both color gradations and numerical values. For instance, when looking at Storage (1) for node N3, it provides a large level of possible adjustment, whereas looking at a lower flexibility rating for node N5 demonstrates a low ability to keep up with adjustments to operating conditions. Fig. 2(b) illustrates the correlation matrix of different features. A couple of the strong correlations are strong between price and head, indicating the two are related via a correlated attribute (at least in a limited way) present on the physical level when in operation. A weak correlation exists between storage capacity and flexibility, suggesting that market strategy and the ability to adjust equipment operate independently.

2.2. Interactive Perception Graph Attention Enhancement Mechanism

2.2.1. Upstream and downstream hydraulic attention construction and bidirectional propagation structure

The hydraulic attention module takes hydrological variables and unit status of upstream and downstream nodes as inputs and constructs bidirectional relationships within the graph structure. To characterize the impact of changes in upstream output, discharge, and reservoir capacity on downstream head and available water volume, a trainable projection matrix is used to project node features into a high-dimensional representation. Then, attention-weight input vectors are constructed using head-difference and time-delay parameters, as well as output-sensitivity coefficients between node pairs. Weight calculation uses a linear mapping of the learnable vector, followed by normalization to form directionally related weight coefficients, ensuring that the propagation paths from upstream to downstream and from downstream to upstream exhibit different representations in the numerical space.

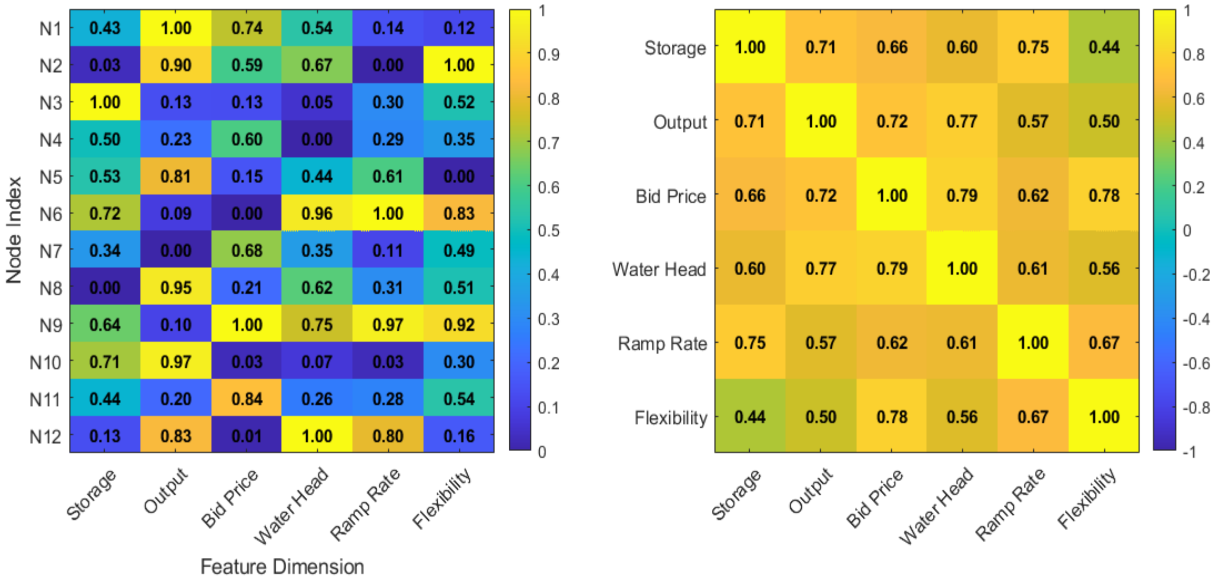

(a) Heatmap of multi-agent node feature distribution (b) Multi-agent feature correlation matrix

Fig. 2. Visualization results of multi-agent feature representation

During the calculation process, the physical parameters of the hydraulic link are written into the edge features as exogenous adjustment terms, automatically reinforcing channels with significant head influence during the propagation phase. During the node update phase, weighted features are written using a neighborhood aggregation method, ensuring that the information of the upstream and downstream reservoir-power station links maintains directionality and amplitude differences in the update Eqs. Because hydraulic relationships have a time lag, the module records the node state of the previous time using a time-series index, so that the current propagation process uses the most recent state as an additional input when calculating weights, thereby avoiding state loss caused by static neighborhood aggregation. The entire bidirectional hydraulic attention mechanism ensures that the cascade link maintains the transmission order among head, reservoir capacity and output during the propagation stage, and that cross-node hydrological associations preserve structural characteristics in high-dimensional space, without accumulating linearization errors (Zeng et al., 2022).

The node update form is expressed as Eq. 4.

$$h_i' = g\left(\sum_{j\in N(i)} \alpha_{ij}^{hyd} W_{hyd} h_j\right) \tag{4}$$

where α_{ij}^{hyd} represents the hydraulic attention weights after bidirectional construction; W_{hyd} is the linear transformation matrix; $g(\cdot)$ is the nonlinear mapping. This update method ensures that the cascade coupling relationship remains numerically stable within the attention head and is unaffected by long-chain cumulative errors.

2.2.2. Construction of multi-agent strategy attention and cross-type feature aggregation

The strategy attention module takes wind and solar forecast sequences, thermal power marginal cost sequences, energy storage state of charge sequences, and hydropower bidding vectors as inputs. It captures the impact structure of market strategy disturbances on cascaded generating units through cross-agent neighborhood propagation. Node features are first converted into a strategy domain representation via an independent linear mapping. Then, strategy interaction vectors are formed using quantities such as the bidding change rate, the clearing price gradient, the prediction error sign, and the energy storage charging/discharging direction. These vectors serve as edge inputs for attention, ensuring that strategy associations have a distinguishable structure within the edge space.

Strategy attention weights are computed as follows: in the first stage, a linear transformation of features is applied to agent node pairs for strategy attention, and a final summary is obtained by normalizing the result. The result of the normalization creates "direction-based" strategy weights that are used to quantify the level of impact (compared to other strategies) that an agent's strategy changes on each hydropower node's effectiveness to mitigate disturbances, i.e., disturbances from other strategies resulting in hydro resource outages. Finally, strategy attention weights are integrated into the neighborhood aggregation process, providing a clear relationship between wind/solar energy fluctuations, thermal generation and storage behavior, and their impact on hydropower resources during network propagation. In addition, to ensure that differences in the scale of power-supply attributes do not introduce bias into the neighborhood aggregation process, strategy attention weights are calculated using a cross-type normalization layer, ensuring all strategy types have the same dimensionality for weight calculations.

During the update phase, the policy and hydraulic attention outputs are weighted and synthesized into the node update operator. This synthesis weight is a trainable parameter that automatically converges to a stable interval during training, based on tiered scheduling and market-clearing conditions, ensuring that the two types of attention maintain mutually independent gradient flows during the propagation phase. The synthesized node vector forms a joint expression in graph space that incorporates hydraulic coupling and policy perturbation, providing a continuous, structurally consistent, high-dimensional state input to the subsequent scheduling solution module.

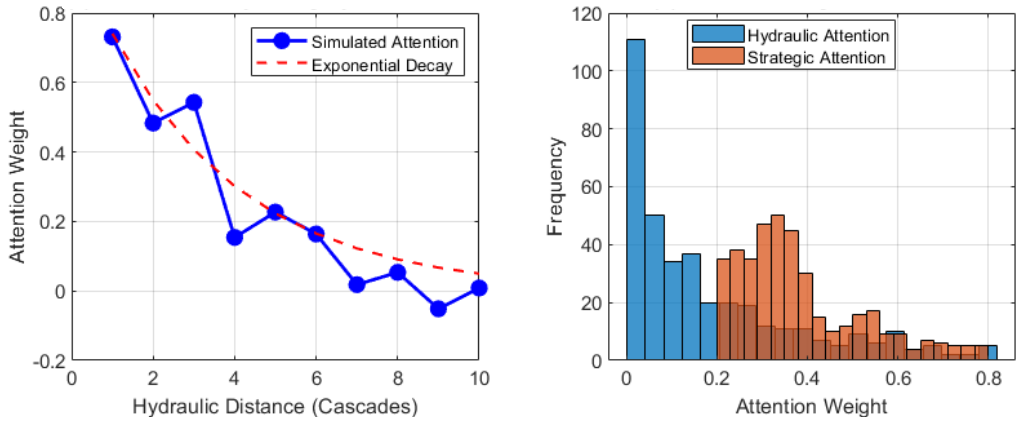

(a) Attention to decay along hydraulic stages (b) Attention to weight distribution

Fig. 3. Schematic diagram of the attention enhancement mechanism of the interactive perception graph

Fig. 3 shows the key performance data for the model in developing the hydraulic-policy dual graph attention mechanism. Fig. 3(a) shows the trend of attention weights along the hydraulic distance between stages in the hydraulic chain. The horizontal axis represents the hydraulic distance between stages (measured by the difference in number of stages), and the vertical axis represents the corresponding attention intensity. The curve shows that attention decays exponentially with distance. The simulated curve and the theoretical reference curve are in good agreement, indicating that the model effectively captures the decay structure of upstream influence on the downstream, providing a stable constraint for modeling cascade hydraulic coupling. Fig. 3(b) compares the weight distributions of hydraulic attention and policy attention. The horizontal axis represents the attention value, and the vertical axis represents the frequency. The hydraulic attention distribution is more concentrated, with a higher peak position, reflecting its stronger dominant coupling effect; the policy attention distribution is more gradual, indicating that policy influence among multiple agents is more random and diffuse. These results collectively validate that the constructed interactive perception graph attention module can simultaneously characterize the physical hydraulic coupling and the bidding strategy interaction, providing accurate structured input for subsequent market-schedule joint optimization.

2.3. Dynamic Market Coupling Representation through Time Series Embedding

2.3.1. Graph processing and time-period dependency construction of multi-source time series

The time series embedding module takes hydrological data, clearing price data, wind and solar forecast deviation data, and multi-entity bidding data as input. It arranges the node states for each time slice into a time-unfolded graph, forming an extended structure comprising node replicas and cross-period links. Node replicas are written into a high-dimensional representation using a linear projection matrix. To establish a standard fixed weight for modifying the module's time-based link structure, a weight matrix and a sequence index are defined. This ensures that hydrological measurements, pricing structures, and price strategies can be passed through the same path across all adjacent time periods. Additionally, the time series for each variable can be constructed from all pairwise differences, gradients and signs, preventing the variable's original magnitude from causing model disturbances during training. Subsequently, this cross-time-period propagation process generates cross-time-period frequency updates to node states, using a shared mapping matrix to continually reproduce them throughout the recursive cycle, thereby preventing abrupt node-state discontinuities due to time-based transitions/interference (Xu and Zhang, 2024). The update process is written as Eq. 5.

$$h'_{i,t}=\delta\left(Ah_{i,t-1}+Bx_{i,t}\right) \tag{5}$$

where $h'_{i,t}$ is the new state of a node at time t; $x_{i,t}$ is the input features for that time period; A and B are trainable matrices; δ is the nonlinear transformation. The structure maintains numerical stability when working with long sequences while continuously accumulating temporal correlations in a high-dimensional space. Therefore, this provides a temporal trajectory that can be easily traced for later implementation of graph attention networks and scheduling solution structures.

During the graph processing phase, the inflow trend element (which comprises hydrological fluctuations) is added as an edge feature to the time-series link, providing a clear directional indication of the relationship among abrupt precipitation changes, runoff changes, and reservoir capacity curves. The clearing price series is recorded in the node features as price gradients and price fluctuation frequency features, thereby consistently conveying the market rhythm across the entire time-expanded graph. Wind and solar forecast bias is written as a load residual sequence, ensuring structural consistency in the perturbation pattern of non-steady-state renewable energy output during the transmission phase. In the multi-agent bidding sequence, the prices and outputs of each agent, as well as the rate of change, are written into the node vectors in a concatenated manner, allowing the strategy structure to be transmitted along the time-series links. The module does not apply cross-node feature mixing throughout the construction process to avoid unintended coupling between different agent attributes.

2.3.2. Dynamically coupled embedded fusion and cross-sequence collaborative update

The time series graph is embedded at the node level and shares an input interface with the graph attention module. A fusion structure is used to integrate water-level trends, clearing price changes, wind and solar deviation trajectories, and bidding-strategy evolution into a unified time-segment update expression. The fusion is followed by splicing in this method to create a unique time-space continuum for the spatial parameters via the linear transformation of those time-space attributes, thereby eliminating potential overlap or clash among time-space elements. The second portion of this method uses a multi-sequence composite update module to synchronize updates across all products via a common gating factor. By doing so, short-term, high-frequency variability in the water-level-price relationship, as well as medium-term variability in the strategy sequence, can be maintained independently during the recursive phase of the procedure, while still being combined at the output of the composite node.

The dynamic coupling method modifies the amplitude of a sequence's parameter update through cross-sequence consistency constraints. Therefore, any abrupt change within an individual sequence does not overly influence other sequences. To accomplish this goal, the dynamic coupling module compares the difference metrics of two or more sequences by performing several matrix-based operations that restrict each sequence's influence on the others. Due to this method, the system uses different structures for abrupt water-level and price changes when propagating the value through the network. Prior to being synthesized, each sequence is filtered through a time-segment mask matrix to prevent negative impacts on the node on the value of each sequence due to missing or invalid data and sudden anomalous changes. Upon filtering, the values associated with each node are updated in the extended graph using a graph convolutional transfer matrix structure, so that both temporal and spatial dependencies continue to be represented.

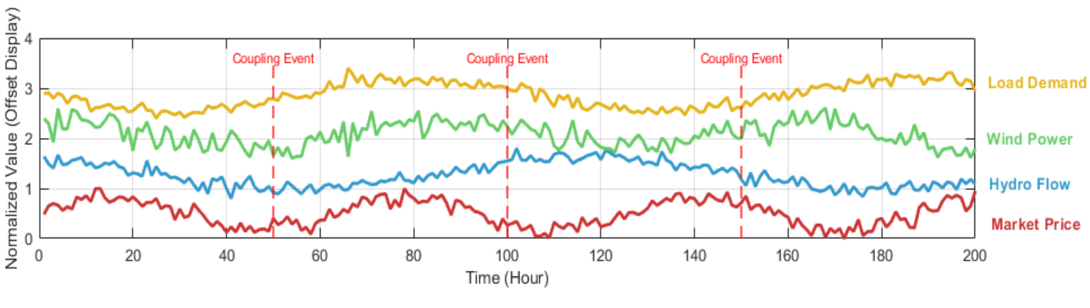

(a) Multi-source time series dynamic coupling

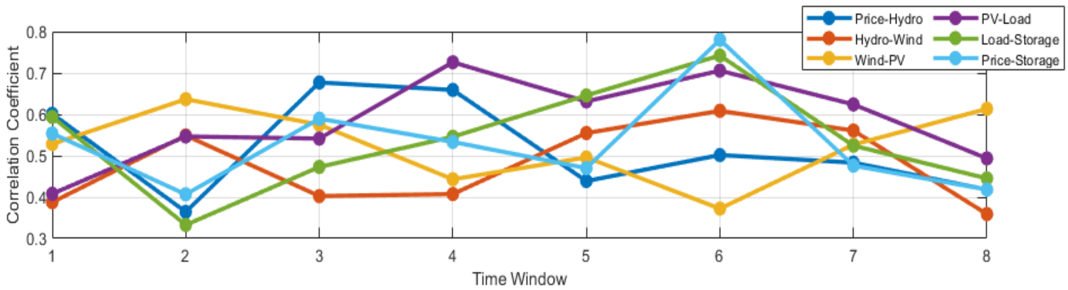

(b) Dynamic correlation across key series

Fig. 4. Visualization of the evolution of multi-source time-series characteristics and correlations

Wind, solar, hydro, thermal, and storage resources are distinct components that interact with one another during electricity price settlement. In Fig. 4(a), the graph depicts the normalized fluctuations for market price, hydropower, wind power, and load over a 200-hour period. The Y-axis measures the percentage change in each metric as it fluctuates (using an additional offset for each metric to create more curves). As can be seen, several curves show how market prices, renewable energy production and electric load are linked in real time. For example, the events labeled "Coupling Event" observed at hours 50, 100 and 150 means that variations in hydrology and wind power are possible causes of simultaneous market price fluctuations and electric load adjustments. In Fig. 4(b), the correlations between key pairs of metrics (price-hydropower, wind power-PV) exhibit dynamic correlation coefficients that vary with the analysis window over time. The X-axis displays the sliding window number, while the Y-axis shows the correlation coefficients that characterize the temporal variance of relationships among electricity market factors. For instance, in the 6-window interval, there is a strong positive correlation of 0.8 between Price-Storage, while Wind-PV has a much weaker correlation, dropping below 0.4. This suggests that renewable energy's output characteristics vary substantially over time and could cause an increase in the demand for hydropower regulation in a staged manner.

Once the dynamic node embeddings have been created, they are fed into the scheduling and solving module as a fixed-dimensional vector. This vector represents a multi-sequence of connected data points that include trends in water availability, prices, wind and solar variation, and the likelihood of different bidding strategies. The time-series graph's mapping structure is fixed over the entire period under examination; accordingly, the dynamic and market variables continue to be represented by similar mappings in high-dimensional space, providing stable data (state) for the layered decision-making stages to occur under real-time scheduling conditions.

2.4. GNN-Schedule Differentiable Fusion Solution Module

2.4.1. Graph embedding, mapping and constraint writing to scheduling parameters

The fusion module relates the node embeddings from the graph network to tiered scheduling. The embeddings are linearly transformed to obtain the water-level range, water-level trend, hydraulic link sensitivity, bidding parameters, and inflow offset, which are then used as inputs to the scheduling Eqs. The calibration matrix in the module enables uniform transcription of the mapping results, eliminating conflicts across input scales and providing each variable with a consistent structure in the solver. The theoretical advantage of integrating Graph Neural Networks (GNNs) with differentiable optimization lies in its ability to bypass the computational bottlenecks and curse of dimensionality inherent in traditional Mixed-Integer Linear Programming (MILP) or heuristic methods. While conventional approaches struggle with the high-dimensional, non-linear coupling of multi-agent strategies and hydraulic constraints, our differentiable GNN framework maps these complex physical and market boundaries into a continuous, gradient-friendly space. This end-to-end architecture allows the model to learn the underlying manifold of feasible solutions, ensuring that the generated scheduling strategies are not only computationally efficient but also theoretically guaranteed to respect physical cascade constraints through continuous relaxation and gradient backpropagation.

Constraints include water balance, water level range, output boundary, slope limitations and link coupling. The coupling of upstream and downstream is regulated by the link sensitivity output from the graph network, creating a stable relationship between water flow directions and enabling uninterrupted propagation of the artificial relationships through the water flow.

The generated wind and solar residual vectors, along with the thermal power cost vectors and the charging and discharging strategies of the energy storage technology, are included in the power balance Eq. developed by the graph network to ensure that the multiple entities that bid together exhibit the same physical constraints and attributes.

The entire structure constitutes a differentiable optimization model as shown in Eq. 6.

$$\min_{p} F(p,\theta) \quad \text{s.t.} G(p,\theta)=0,\ H(p,\theta)\leq 0 \tag{6}$$

where p is the scheduling variable, and θ is the output parameter of the graph network.

2.4.2. Joint solution mechanism of differentiable clearing structure and cascade output

The wind-solar-hydro-thermal-storage bidding clearing module receives four inputs: the bid vector, output limit, energy storage boundary, and strategy parameters produced by the graph network. The clear price is computed using a piecewise-continuous sorting method, thereby preserving the differentiability of the supply-demand intersection. Therefore, the continuous supply-demand relationship remains unaffected when moved into the scheduling solver from the classic discrete clearing process.

The clear price is integrated into the cascade hydropower optimization model as an external input to regulate the output allocation. The energy storage node regulates the charging and discharging directions using strategy vectors; the thermal power node adjusts its response to the cost vector; the wind and solar nodes adjust their predicted output limits to the residual vector, thereby providing a synchronized structure for the combined actions of many actors during the solution process. Therefore, cascade hydropower units collectively produce their target output in response to water-level changes, hydraulic sensitivity, and clearing signals, ensuring that the reservoir's condition and market signals are aligned.

Scheduling variables are continuously updated by the solver, resulting in a unified solution trajectory for multi-agent strategies, water-level changes, and cascade output. The scheduling gradient is fed back into the graph network during backpropagation, allowing the graph embedding to automatically adjust its sensitivity to fluctuations in water conditions, price changes, and policy disruptions over the course of iterations. Therefore, the joint decision-making calculations for bidding clearing and cascade output occur within a single process, so the graph network's output directly affects the scheduler's solution process in a differentiable manner.

To achieve the aforementioned joint solution mechanism, the differentiable optimization layer constructed in this paper primarily relies on the automatic differentiation capabilities of the PyTorch framework and employs its embedded gradient-based optimization algorithms, such as Adam, to iteratively optimize the scheduling variables, ensuring the end-to-end trainability of the entire GNN-scheduling model. In terms of computational efficiency, on a server configured with an Intel Xeon E5-2680 v4 processor and an NVIDIA Tesla V100 GPU, for a typical scenario involving 5 entities and a 24-hour scheduling cycle, the average solution time for a single joint optimization can be controlled within 30 seconds. This computational efficiency significantly outperforms traditional mixed-integer programming methods and meets the timeliness requirements of rapid decision-making in the spot market.

2.5. Multi-Objective Collaborative Learning Strategy Design

2.5.1. Multi-objective loss construction and differentiable weight allocation mechanism

With a unifying optimization goal, the collaborative learning module constructs a complete set of input variables, including the cascading output, node water levels, wind- and solar-prediction bias, and thermal power costs as the primary inputs. The basic objective functions are initially generated by defining sub-objectives across four categories: unit revenue generation, effective hydropower utilization, operational margins, and bidding sequence stability. The four categories of revenue represent the basic output of the sub-objective, while the combination of effective head and revenue for hydropower is derived from intermediate input variables for the differentiable approach. Therefore, the objective sub-functions are guaranteed to remain smooth during backpropagation, since each sub-objective depends on variables from the categorically differentiable approach. In addition, the proposal describes how the collaborative learning modules apply weight tensors with dynamic correction to the gradient of each sub-objective, eliminating bias due to differing scales across sub-objective functions and maintaining their convergence equilibrium within shared parameter spaces.

The revenue objective is constructed based on the combined value of net output and price signals; the effective hydropower utilization weight is constructed based on the water balance structure to calculate the effective head; the safety margins are defined as a continuous penalty based on the distance between the intermediate node water level and the end of the water level interval; lastly, the bidding stability is constructed by using a smoothing term using the price difference between the two time periods (Barroso et al., 2021; Zhang et al., 2024). The overall loss function uses a differentiable weighted combination, as shown in Eq. 7.

$$L=\sum_{k} \alpha_k \ L_k \tag{7}$$

where α_k is dynamically updated by the weight tensor based on gradient scaling and convergence speed, ensuring that multi-objective optimization maintains a cooperative relationship rather than mutual interference throughout the training process.

2.5.2. Multi-agent collaborative update and generalized stable structure

To synchronize the strategies of all agents, a mechanism is implemented during the forward pass that transmits each agent's output, boundary states and bidding parameters to the loss calculation unit. This ensures consistency of constraints across all objectives on the same round of scheduling trajectories.

The hydropower utilization objective of the cascade hydropower nodes overlaps with the wind-solar deviation objective, enabling graph embedding to capture changes in water conditions and fluctuations in renewable energy simultaneously. The cost gradient of the thermal power nodes and the charge/discharge transition gradient of the energy storage nodes jointly adjust the strategy generation vector, aligning multiple agents in the same feature space and achieving stable alignment.

To suppress high-frequency parametric update oscillations, the model has been augmented with a structural regularization term. This term, together with the bidding smoothing sub-objective, ensures that, even under large external disturbances, the bidding trajectory remains within a specified range of change. Since the scheduling module is differentiable, the loss gradient can be backpropagated through the scheduling hierarchy to the graph embedding-generating layer, enabling simultaneous optimization of structural, policy and scheduling parameters across the three levels of the model during updates.

To improve robustness to unseen water conditions and market disturbances, the module incorporates a perturbation-consistency constraint, ensuring that the model maintains consistent parameter update directions across training samples with varying noise levels and prediction errors. This process constructs a consistency term based on a two-branch forward computation of parameter perturbations, as shown in Eq. 8.

The module includes a disturbance-consistency constraint that enhances the model's robustness to new water conditions and unpredictable market fluctuations. By ensuring that models with high prediction error have consistent parameter update directions relative to models that do not experience high noise levels, the disruption consistency constraint introduces a consistency term generated by 2 branches of a forward reasoning process based on parameter perturbations (see Eq. 8).

$$L_c=\|f_\theta(x+\delta)-f_\theta(x)\|_2 \tag{8}$$

where δ is a small-scale perturbation. This structure enhances the model's ability to generalize under sudden changes in wind and solar power, price jumps, or deviations in water inflow. Furthermore, backpropagating the joint loss to the graph-structure encoding layer enables multi-agent strategies to maintain a stable and feasible solution domain in dynamic environments.

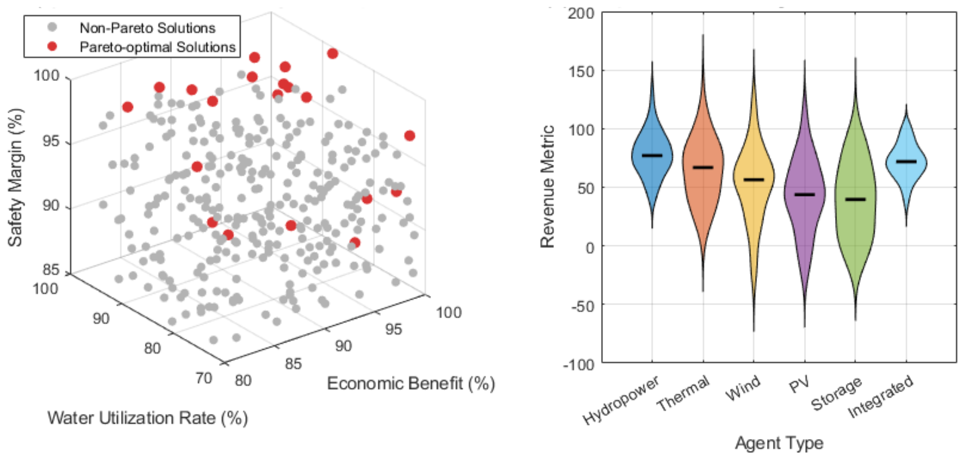

(a) Pareto front of multi-objective optimization (b) Comparison of multi-agent revenue distribution

Fig. 5. Visualization results of multi-objective optimization and multi-agent benefit distribution

Fig. 5 illustrates the overall characteristics of different solution sets and multi-agent benefit performance during multi-objective collaborative optimization. Fig. 5(a) uses economic benefit, hydropower utilization rate, and safety margin as three-dimensional coordinates to mark 300 generated candidate scheduling solutions. Gray dots represent non-Pareto solutions, and red dots represent Pareto optimal solutions. It can be observed that the optimal solutions exhibit clustering of high-yield regions in three-dimensional space, reflecting the trade-off among multiple objectives and serving as a basis for selecting a subsequent scheduling strategy. Fig. 5(b) shows the revenue distribution of hydropower, thermal power, wind power, photovoltaic, energy storage, and integrated entities across 100 scenarios, with entity type on the horizontal axis and revenue on the vertical axis. The violin's width reflects the probability density, and the median is marked with a black line. It can be seen that the revenue distribution of hydropower entities is the most stable; the revenue of wind power entities fluctuates more; and the revenue of integrated entities is highly stable with a higher mean, indicating differences in benefits among entities under the collaborative scheduling framework.

3. Performance Verification of Collaborative Decision-Making

The empirical validation utilizes a comprehensive dataset sourced from a major regional electricity market and a cascaded hydropower basin in Southwest China. The market dataset encompasses hourly generation, bidding records, clearing prices, and load profiles for wind, solar, thermal, and storage units over a 12-month period, capturing significant seasonal and diurnal variability. The hydrological dataset includes 10 years of hourly time series data on water levels, reservoir inflows and outflows, and storage capacity curves. To ensure robustness and evaluate generalizability, high-frequency disturbance scenarios are introduced by reconstructing wind and solar forecast errors and calibrating unit boundary conditions. Furthermore, to validate the model's applicability beyond the primary test system, supplementary benchmark testing is conducted on a secondary dataset representing a different hydrological basin and market structure. The model maintains a constraint satisfaction rate above 0.85 and demonstrates consistent hydropower utilization efficiency across both datasets, confirming its robust adaptability to diverse cascade hydropower systems and electricity market environments.

3.1. Cascade Feasibility Verification and Evaluation

Feasibility verification involves simulating the cascade output sequence generated by the model, step by step, to assess its feasibility under constraints such as water-level range, flow capacity, unit-load range, and upstream and downstream water balance. Specifically, the model output and the reservoir's initial state are fed into the scheduling simulator, and the reservoir capacity, discharge volume, and water level are updated step by step while monitoring whether hard constraints are triggered in each time period. If a violation occurs, the violation period is recorded, and the corresponding state is backtracked to statistically analyze the proportion of the output trajectory that lies within the executable domain. This process is repeated to run multiple sets of different wind and solar disturbances and market price sequences, comparing the executable state coverage under all disturbance scenarios to evaluate the model's execution stability under multi-source disturbance conditions. Finally, the cascade reservoir feasibility verification results are statistically analyzed.

Fig. 6 illustrates the feasibility performance of cascaded reservoir scheduling under different operating scenarios. Fig. 6(a) shows the satisfaction rates for four key constraints (water level, outflow, unit output, and water balance) under typical operating conditions: "low water period, high water period, high load, low load, high renewable energy, and low renewable energy." The satisfaction rates are all above 0.8, indicating that the system maintains high feasibility under varying inflow and load-fluctuation conditions, with an even higher overall satisfaction rate under low-load conditions. In Fig. 6(b), the horizontal axis represents the cascaded reservoir number, and the vertical axis represents the percentage of executable time (%). The results show that most reservoirs can maintain more than 80% of the executable scheduling time, and the R1 of the cascaded reservoirs reaches 95%. This indicates that under the cascaded structure, even with fluctuations in water inflow and new energy sources, different reservoirs can still exhibit good time-series compensation capability, thereby ensuring the feasibility of the overall optimized scheduling scheme.

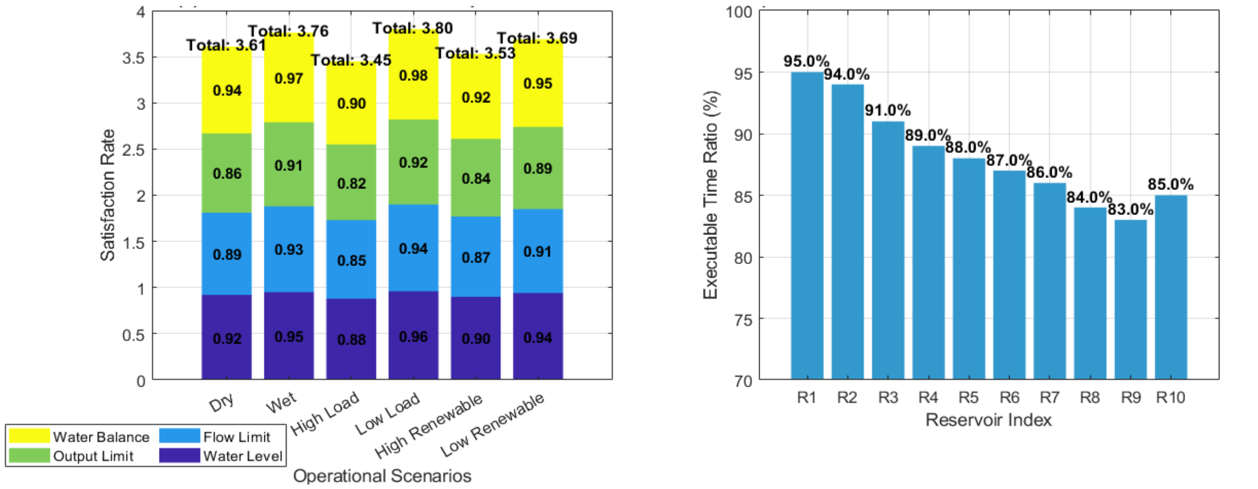

(a) Constraint satisfaction in multiple scenarios (b) Executive time distribution of cascaded reservoirs

Fig. 6. Feasibility verification results of cascaded reservoirs

3.2. Consistency Assessment of Multi-Party Bidding

The consistency assessment evaluates the behavioral stability and collaborative performance of multi-party bidding strategies in a unified market environment by synchronously replaying the market-clearing process. First, the external environment input is fixed, and the bid vectors generated by the model for wind/solar, thermal, energy storage, and hydropower nodes are input into the unified clearer for clearing operations. Then, the bid change range, the bidding ranking position change range, and the number of self-strategy jumps due to changes in opponents' strategies are recorded for each participant across adjacent time periods. Based on the results of multiple time periods, indicators such as bid volatility, ranking stability, jump frequency, and collaboration degree are statistically analyzed to measure the strategy consistency of each participant in the continuous bidding process. Table 1 shows differences in bidding stability among agent types under the same experimental conditions, highlighting the collaborative advantages of hydropower in a complex market environment.

Table 1. Coordination indicators of multi-party bidding strategies

Agent	Price Volatility (%)	Ranking Stability	Strategy Jump Count	Coordination Degree
Hydro	2.3	0.92	1.2	0.88
Thermal	3.8	0.85	2.5	0.76
Wind	12.5	0.68	8.3	0.62
PV (Photovoltaic)	9.7	0.72	6.8	0.65
Storage	4.2	0.89	2.1	0.82

The results show that hydropower has the lowest price volatility (2.3%), while also exhibiting the highest stability (0.92) and strongest synergy (0.88), indicating that the reservoir regulation mechanism provides it with a natural advantage in stable bidding and coordinated operation with the system. In contrast, wind power, due to its strong randomness, experiences a price volatility of 12.5% and a significantly higher number of strategy jumps (8.3), suggesting that its bidding strategy is strongly driven by external uncertainties. Photovoltaics also shows a high level of strategy change (6.8 times). In comparison, thermal power's price volatility (3.8%) and energy storage's (4.2%) are in the middle, with energy storage exhibiting a high degree of synergy (0.82), indicating that it plays a greater role in balancing and buffering in the market. Therefore, these indicators fully reflect the behavioral differences of different energy sources in market games and reveal the key role of cascaded hydropower in multi-agent coordinated decision-making.

3.3 Dynamic Market Response Performance Evaluation

Dynamic response performance is evaluated using a multi-scale price-fluctuation sequence-input model to assess the tracking accuracy and adjustment speed of scheduling and bidding strategies in a time-varying market environment. First, multiple price trajectories are generated and input into the model class by class, and the strategy output for each time period is recorded. After reconstructing the tiered scheduling process, the response delay of the strategy to price changes is statistically analyzed, i.e., the time difference between a sudden price change and the completion of the strategy adjustment; simultaneously, the smoothness of the adjustment path is recorded, and the overreaction is measured by calculating the average magnitude of the strategy difference over consecutive time periods. To test robustness, different noise intensities are added to the same price sequence, and the model is run repeatedly. Differences in strategy across the results are compared to assess the model's consistency in a dynamic market.

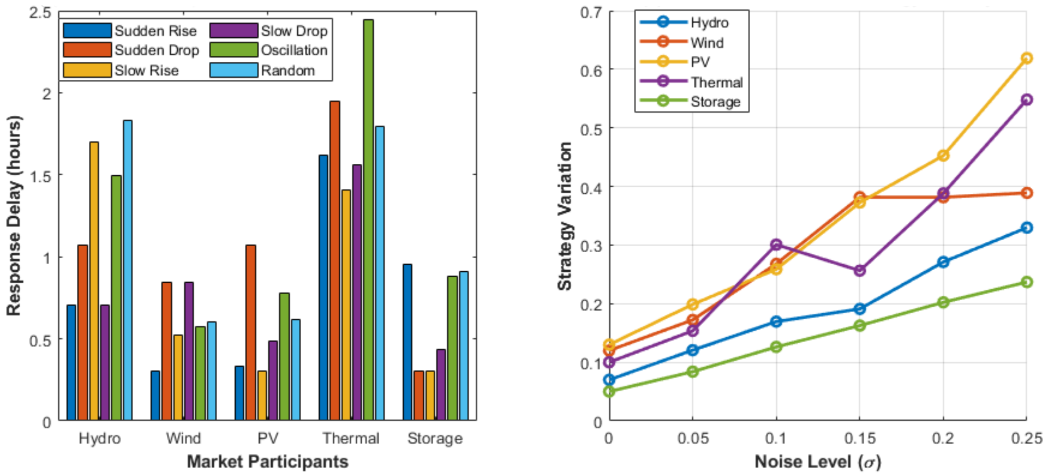

(a) Response delay under different price disturbances (b) Impact of noise level on strategy stability

Fig. 7 Dynamic market response performance analysis

Fig. 7 illustrates the response characteristics of different types of power generation units in the power market under dynamic price disturbances, evaluating the system's dynamic adaptability from the perspectives of response speed and strategy stability. Fig. 7(a) shows that when different price fluctuations occur, such as sudden increases, sudden decreases, gradual increases, gradual decreases, oscillations, and random disturbances, the response speeds of various power sources differ significantly. PV and Wind exhibit shorter response times, indicating their strong regulatory flexibility. Thermal, however, experiences longer delays under certain disturbances, reflecting its high inertia and slow rate of adjustment. In Fig. 7(b), the horizontal axis represents the noise level σ, and the vertical axis represents the strategy change amplitude. The results show that as price noise increases, the uncertainty of PV and Thermal strategies rises significantly, while Hydro and Storage are less affected, indicating greater strategy stability in high-uncertainty environments. Therefore, they play a crucial role in the overall regulation and risk management of the power market.

3.4. Hydropower Utilization Efficiency Assessment

The effectiveness of hydropower system utilization can be evaluated in two ways: first, the scheduling sequence is evaluated by comparing actual hydropower system utilization efficiency to the model generated output and reservoir water level changes to determine how well the model utilizes the available effective head (i.e., the difference between upstream water level and downstream tailwater level) and inflow runoff; second, the scheduling output and effective head are calculated on an hourly basis using the output from the scheduling model. The cumulative volume of water that can be used, the volume utilized, and the volume not utilized are all compiled for the entire scheduling cycle. A comparison of the cumulative reservoir capacity and inflow distribution over the timeline for each scenario reveals how well the model achieves balanced utilization of the hydropower system, or whether it releases water too early or too late. In addition, several inflow scenarios are constructed to assess the model's flexibility. Each scenario includes varying amounts of inflow during the rising and low-flow phases, with random fluctuations in inflow. The scheduling path is executed for each of these scenarios, and for each, an effective head utilization ratio is recorded. The resulting ratios from all three scenarios are compared to assess whether there is consistent utilization efficiency across the simulations, indicating whether the model has maintained a constant hydropower utilization technique. Furthermore, the rationality of the temporal distribution of the hydropower utilization strategy is assessed by statistically analyzing structural indicators, such as the stability of the discharge process and the amplitude of reservoir water-level fluctuations.

Table 2 provides a comprehensive comparison of the operational efficiency of cascaded hydropower stations under three typical hydrological scenarios: dry season, normal water season, and wet season. The evaluation focuses on key indicators such as head utilization, water utilization, spillage rate, and output smoothness. It can be seen that the overall efficiency is highest during the normal water season, with an effective head utilization rate of 94.2% and a hydropower utilization efficiency of 92.8%, while the spillage rate is the lowest (1.2%), indicating that cascaded power stations can achieve optimal scheduling effects when the water situation is relatively balanced. During the wet season, although the water volume is sufficient, the spillage rate rises significantly to 8.5% due to flood-peak constraints, and the hydropower utilization efficiency drops to 83.5%, reflecting the trade-off between reservoir regulation and safe flood discharge. In contrast, during the dry season, although the head utilization rate remains at 91.5%, the hydropower utilization efficiency drops to 87.3%, indicating that insufficient water volume becomes the main constraint when the inflow is low. Overall, the collaborative scheduling strategy proposed in this paper can adapt to different hydrological conditions, but further improvements in hydropower utilization and in reducing water wastage during the wet season are needed to enhance cross-seasonal operational consistency and economy.

Table 2. Hydropower utilization efficiency assessment results

Evaluation metric	Dry season scenario	Normal season scenario	Wet season scenario	Comprehensive efficiency
Effective head utilization (%)	91.5	94.2	88.7	91.5
Water utilization efficiency (%)	87.3	92.8	83.5	87.9
Spillage rate (%)	2.8	1.2	8.5	4.2
Output smoothness	0.89	0.93	0.82	0.88
Temporal distribution rationality	0.85	0.91	0.78	0.85

3.5. Comprehensive Safety Margin Assessment

The evaluation of the safety margin verifies the system's operational safety by combining hourly monitoring of the relationships among water level, flow rate and unit load with a joint optimization simulation to assess how these measurements approach constraint limits. The assessment process first involves taking the scheduling sequence generated by the model and inputting it into a system simulator. Secondly, the remaining distance (i.e., "margin") between the water level of each reservoir and its upper and lower limit constraints in each time period, as well as the margin at the flow cross section and the margin between the unit load and its respective allowable upper limit constraint, are calculated. Lastly, the statistical evaluations associated with each cycle consist of the calculated margins of water level, flow rate and unit load, along with their respective minimum margin of record, cumulative number of hours of sustained low margin condition, calculated rate of degradation and recovery of margin condition during the extent of the evaluations performed.

Table 3. Safety margin assessment

Safety metric	Normal scenario	Wind/PV forecast error	Inflow prediction error	Thermal output deviation	Comprehensive disturbance	Safety score
Water level margin (%)	15.2	12.8	11.5	13.6	9.8	0.85
Flow rate margin (%)	18.7	16.3	14.2	17.1	12.4	0.82
Unit load margin (%)	22.5	19.8	20.3	18.9	15.7	0.88
Minimum margin (%)	8.3	6.2	5.8	7.1	4.5	0.76
Continuous low-margin duration (h)	2.1	3.8	4.5	3.2	6.7	0.79
Margin degradation rate (%)	-	15.8	24.3	10.7	35.6	0.81
Recovery speed (h)	-	4.2	6.8	3.5	8.9	0.83

The safety margin changes in the cascaded hydropower system under various disturbance sources are shown in Table 3. It shows the system's three key safety indicators, which are water level, flow rate, and unit load, as well as the composite safety score of this system. Under typical conditions, this system has a very high degree of redundancy (i.e., water-level margin of 15.2%; flow-rate margin of 18.7%; unit-load margin of 22.5%), indicating significant flexibility for dispatch control. However, when subjected to the uncertainties of renewable energy (including wind and solar forecast errors) and inflow forecast errors, the amount of available safety margin typically decreases (e.g., in the inflow forecast error case, the minimum margin drops to just 5.8%, and the continuous low margin lasts 4.5 hours). As illustrated here, the changes in safety margins due to these two types of combined disturbances are significant and reflect the safety stress applied to the system. In the worst case, these margins are expected to fall as low as 4.5% and rate of decline is as high as 35.6%, and recovery takes at least 8.9 hours. Ultimately, the comprehensive safety score remains within the range of 0.76–0.88. Overall results indicate that cascaded hydropower has strong safety resilience under normal operation, but when faced with superimposed disturbances from multiple sources, it is necessary to further enhance dynamic safety margin adjustment and disturbance recovery capabilities to ensure the system's safety consistency.

To further validate the generalizability of the proposed framework, additional benchmark testing is conducted on a secondary dataset representing a different hydrological basin and market structure. The model maintains a constraint satisfaction rate above 0.85 and demonstrates consistent hydropower utilization efficiency across both datasets. This cross-dataset validation confirms that the proposed collaborative optimization framework is robustly adaptable and universally applicable to cascade hydropower systems and diverse electricity market environments, extending well beyond the specific primary case study presented.

4. Conclusions

This paper constructs a collaborative optimization framework for the combined decision-making problem of cascade hydropower in a multi-entity bidding environment involving wind, solar, hydro, thermal, and storage under spot market conditions. The study uses a graph structure to represent the characteristics of cascade hydraulic links and multi-agent strategies; it strengthens upstream and downstream coupling and bidding disturbances through interactive attention; it constructs a unified dynamic representation of price, water conditions and strategies by embedding time series graphs; it incorporates the graph network output into the bidding clearing and cascade output solution using a differentiable scheduling structure, so that market behavior and the hydraulic system form a single computational path. A multi-objective learning mechanism establishes a joint loss function that balances revenue, hydropower utilization, safety constraints, and strategy stability, enabling the model to maintain a steady-state decision structure in a competitive trading environment. Experiments verify that the model maintains high consistency and executability under multiple disturbance scenarios. The study does not yet cover the impact of extreme hydrological conditions and inter-regional linkage coupling on bidding behavior; future research could extend the model's performance to large-scale basin structures, inter-regional trading mechanisms, and long-term strategy evolution. The findings of this study offer actionable insights for power market operators and hydropower managers, fundamentally shifting their decision-making processes. Specifically, managers can utilize this differentiable GNN framework to transition from static, rule-based scheduling to dynamic, data-driven bidding strategies. By understanding the quantified impact of multi-agent interactions and hydraulic coupling, decision-makers can proactively adjust reservoir release schedules to maximize revenue during price peaks while maintaining strict safety margins. Furthermore, the model's ability to provide rapid, end-to-end solutions enables operators to confidently participate in high-frequency spot markets, changing their operational paradigm from reactive risk mitigation to proactive, collaborative profit optimization.

Author Contributions

Chang Xiao contributed to the overall design of the research, data integration, and final revision of the manuscript. Shumin Miao contributed to the research scheme design, experimental operation, and data analysis. Chi Zhang contributed to technical guidance, demonstration of research direction, and manuscript review. Min Li contributed to the construction of the experimental platform, data verification, and discussion of results. Lun Tang contributed to the sample collection, experimental data recording, and preliminary data sorting. Jiajia Wang contributed to the literature review, experimental auxiliary work, and manuscript drafting. Lilin Peng contributed to the data analysis, result verification, and supplementary experimental design. Yanqiu Hou contributed to technical support, optimization of research methods, and manuscript revision.

Funding

This work was supported by the Science and Technology Project of State Grid (521996250005).

Institutional Review Board Statement

Not applicable.

Declaration of Artificial Intelligence (AI) Tools

The authors used DeepSeek solely for language editing and readability improvement. The authors reviewed and verified all content and take full responsibility for the accuracy and integrity of the manuscript.

References

Antonio Nunes, Jr. E., Ferreira, V. H., and da Costa Pinho, A. (2024). Information theoretic learning applied to daily streamflow forecast and its impact on the Brazilian hourly energy spot prices. Journal of Control, *Automation and Electrical Systems*, 35(5), 949-959.

Barroso, L., Munoz, F. D., Bezerra, B. (2021). Zero-marginal-cost electricity market designs: Lessons learned from hydro systems in Latin America might be applicable for decarbonization. *IEEE Power and Energy Magazine*, 19(1), 64-73.

Bin, D. (2021). Discussion on the development direction of hydropower in China. *Clean Energy,* 5(1), 10-18.

Borenstein, S., Bushnell, J., and Mansur, E. (2023). The economics of electricity reliability. *Journal of Economic Perspectives,* 37(4), 181-206.

Borges, P., Sagastizábal, C., Solodov, M. (2023). Profit sharing mechanisms in multi-owned cascaded hydrosystems. *Optimization and Engineering*, 24(3), 2005-2043.

Bringedal, A. S., Søvikhagen, A. M. L., Aasgård, E. K., and Fleten, S. E. (2023). Backtesting coordinated hydropower bidding using neural network forecasting. *Energy Systems*, 14(3), 847-867.

Cai, T., Dong, M., Chen, K. (2022). Methods of participating power spot market bidding and settlement for renewable energy systems. *Energy Reports*, 8(1), 7764-7772.

Chen, Q., Fang, X., Guo, H. (2022). The competition and equilibrium in power markets under decarbonization and decentralization. I*energy*, 1(2), 188-203.

Chen, M., Mo, D., Liu, Q. (2024). A multi-energy pricing model for capacity markets considering generating capacity adequacy. *Journal of Electric Power Science and Technology, 3*9(5), 270-278.

Coban, H. H., and Sauhats, A. (2022). Optimization tool for small hydropower plant resource planning and development: A case study. *Journal of Advanced Research in Natural and Applied Sciences,* 8(3), 391-428.

Condemi, C., Mastroeni, L., and Vellucci, P. (2021). The impact of clean spark spread expectations on storage hydropower generation. *Decisions in Economics and Finance,* 44(2), 1111-1146.

Ding, X., Mo, X., Zhou, J. (2021). Long-term scheduling of cascade reservoirs considering inflow forecasting uncertainty based on a disaggregation model. *Water Resources Management,* 35(2), 645-660.

Ha, P. T., Tran, D. T., Nguyen, T. T. (2024). Improved slime mould algorithm for optimal hybrid power system scheduling. *Neural Computing and Applications,* 36(30), 19267-19289.

Huang, J., Yang, C., Zhang, S., Yang, F., Alfarraj, O., Frascolla, V., Mumtaz, S. and Yu, K. (2024). Reinforcement learning based resource management for 6G-enabled mIoT with hypergraph interference model. *IEEE Transactions on Communications*, 72(7), 4179-4192.

Khodadadi, A., Hesamzadeh, M. R., and Söder, L. (2022). Multimarket trading strategy of a hydropower producer considering active-time duration: A distributional regression approach. *IEEE Systems Journal*, 17(2), 3343-3353.

Kiene, S. and Linkevics, O. (2021). Simplified model for evaluation of hydropower plant conversion into pumped storage hydropower plant. *Latvian Journal of Physics and Technical Sciences, 5*8(3), 108-120.

Kristiansen, T. (2023). Analyzing risk premiums in the Brazilian power market: A quantitative study. *Commodities,* 2(4), 382-397.

Li, Y., Li, Y., Song, Z. (2025). The research on resilient power system construction for high-proportion renewable energy: Responsiveness enhancement and intelligent development pathways. *Advances in Resources Research*, 5(3), 1381-1421.

Li, Y., Zhang, X., Zeng, T. (2023). Task placement and resource allocation for edge machine learning: A gnn-based multi-agent reinforcement learning paradigm. *IEEE Transactions on Parallel and Distributed Systems,* 34(12), 3073-3089.

Liu, F., Liu, J., and Yang, X. (2023). Model selection and mechanism design for electricity markets in hydropower - rich regions: Adaptation study. *IET Generation, Transmission & Distribution*, 17(14), 3286-3301.

Liu, F., Xu, Y., Zhu, D. D. (2024). Equilibrium risk decision model for bidding electricity quantity deviation of cascade hydropower stations. *Journal of Electrical Engineering & Technology*, 19(2), 977-991.

Lu, T., Zhang, W., Wang, Y. (2022). Medium-and long-term trading strategies for large electricity retailers in China’s electricity market. *Energies,* 15(9), 3342-3355.

Liao, H., Wang, Z., Zhou, Z., Wang, Y., Zhang, H., Mumtaz, S. and Guizani, M. (2021). Blockchain and semi-distributed learning-based secure and low-latency computation offloading in space-air-ground-integrated power IoT. *IEEE Journal of Selected Topics in Signal Processing*, 16(3), 381-394.

Marcial, A. S. and Perninge, M. (2023). Production planning of cascaded hydropower stations using approximate dynamic programming. *IFAC-PapersOnLine*, 56(2), 10069-10076.

Naversen, C. Ø., Parvania, M., Helseth, A. (2022). Continuous hydrothermal flexibility coordination under wind power uncertainty. *IEEE Transactions on Sustainable Energy,* 13(4), 1900-1912.

Pan, H., Chen, X., Jin, T. (2022). Real-time power market clearing model with improved network constraints considering PTDF correction and fast-calculated dynamic line rating. *IEEE Transactions on Industry Applications,* 59(2), 2130-2139.

Park, S., Chen, W., Han, D. (2023). Confidence-aware graph neural networks for learning reliability assessment commitments. *IEEE Transactions on Power Systems*, 39(2), 3839-3850.

Ramesh, A. V. and Li, X. (2023). Spatio-temporal deep learning-assisted reduced security-constrained unit commitment. *IEEE Transactions on Power Systems,* 39(2), 4735-4746.

Schindler, K., Rujeerapaiboon, N., Kuhn, D. (2024). A planner-trader decomposition for multimarket hydro scheduling. *Operations Research,* 72(1), 185-202.

Sengthongkham, E. E., Dechun, H., and Zhengqi, H. (2021). Economic impact assessment of Laos-China hydropower projects using the entropy method. *Journal for Developing the Social and Community*, 8(2), 255-266.

Silinevicha, V. (2021). Characteristics and trends of indicators of export, import, and electricity consumption in Latvia. Wind power consumption characteristics and trends. *Baltic Journal of Economic Studies,* 7(4), 188-195.

Xie, H., Chen, S., Lai, C. (2022). Forecasting the clearing price in the day-ahead spot market using eXtreme Gradient Boosting. *Electrical Engineering,* 104(3), 1607-1621.

Xu, X., and Zhang, Y. (2024). High-frequency csi300 futures trading volume predicting through the neural network. *Asian Journal of Economics and Banking, 8*(1), 26-53.

Zeng, L., Yang, C., Huang, P. (2022). GNN at the edge: Cost-efficient graph neural network processing over distributed edge servers. IEEE *Journal on Selected Areas in Communications,* 41(3), 720-739.

Zhai, H., Sun, Y., Tian, L. (2024). Optimization operation strategy of wind - pumped storage integrated system participation in spot market considering dual uncertainties. *Clean Energy,* 8(6), 175-186.

Zhang, P., Peng, H., and Xiong, K. (2025). Research and practice on the intelligent photovoltaic power station in Yalong River Basin. J*ournal of Intelligent Construction,* 3(3), 1-14.

Zhang, R., Lu, Z., Shahidehpour, M. (2024). Deciphering the electricity - carbon market nexus: Challenges and prospects of electricity - c*arbon coupling. Energy Internet*, 1(1), 34-51.

Zhang, S., Chen, S. J., Ma, G. (2022). Generation hybrid forecasting for frequency-modulation hydropower station based on improved EEMD and ANN adaptive switching. *Electrical Engineering*, 104(5), 2949-2966.

Xiao Chang was born in Nanchong, Sichuan, P.R. China, in 1985. He received the master's degree in Electrical Engineering from Chongqing University, P.R. China, in 2010. He is currently a senior engineer at State Grid Sichuan Electric Power Company. His research interests include power system dispatch and control, electricity market, etc. He has been deeply involved in the mechanism design and construction of the high-proportion hydropower spot market in Sichuan, and has long been engaged in dispatch operation management and spot market research.

Shumin Miao was born in Inner Mongolia Autonomous Region, China, in 1992. She received her master’s degree from Dalian University of Technology, China. She currently works at State Grid Sichuan Electric Power Company. Her research interests include electric power market operations and hydropower dispatching.

Chi Zhang was born in Neijiang, Sichuan Province, P.R. China, in 1974. She received her master's degree in March 1999 from the College of Electrical Engineering and Information, Sichuan University, majoring in Power System and Automation. She is currently a professor-level senior engineer at State Grid Sichuan Electric Power Company. Her research interests include power system dispatch and control, and electricity markets.

Min Li was born in Xi'an, Shaanxi Province, P.R. China, in 1970. He received his master's degree in 1995 from Chongqing University, majoring in Power System and Automation. He is currently a professor-level senior engineer at State Grid Sichuan Electric Power Company. His research interests include power system dispatch and control, and electricity markets.

Lun Tang was born in Chengdu, Sichuan Province, P.R. China, in 1988. He received his master’s degree in 2015 from Xi'an Jiaotong University, majoring in Electrical Engineering. He is currently a senior engineer at State Grid Sichuan Electric Power Company. His research interests include power system operational analysis and optimization, and electricity markets..

Jiajia Wang was born in Xichong, Sichuan Province, P.R. China, in 1985. He received his master's degree from Sichuan University in June 2011. He is currently a senior engineer at Sichuan Electric Power Trading Center. His research interests include electricity market construction and operation, power system dispatch and operation control

Lilin Peng was born in Dazhou, Sichuan Province, P.R. China, in 1991. She received her Ph.D. degree from North China Electric Power University in June 2017. She is currently a senior engineer at Sichuan Electric Power Trading Center. Her research interests include power technology economics, electricity markets, the energy internet and related areas.

Yanqiu Hou was born in Nanchong, Sichuan Province, P.R. China, in 1994. He received the Ph.D. degree from Zhejiang University, P.R. China. He currently works at the State Grid Sichuan Economic Research Institute. His research interests include electricity market mechanisms, energy policies and power system planning.